Radial excitation states of η and η′ in the chiral quark model*

CHEN Shao-Na(陈绍娜)[1] PING Jia-Lun(平加伦)[1,2;1)]

[1] School of Physical Science and Technology, Nanjing Normal University, Nanjing 210097, China
[2] School of Physics and Microelectronics, Shandong University, Jinan 250100, China

Abstract: A chiral quark model is applied to calculate the spectra of pseudoscalar mesons η and η′. By analyzing the obtained spectra, we find that the mesons $\eta'(2\,^1S_0)$, $\eta(4\,^1S_0)$, $\eta'(3\,^1S_0)$ and $\eta'(4\,^1S_0)$ are the possible candidates of η(1760), X(1835), X(2120) and X(2370). The strong decay widths of these pseudoscalars to all the possible two-body decay channels are calculated within the framework of the $^3P_0$ model. Although the total width of $\eta'(2\,^1S_0)$ is compatible with the BES Collaboration's experimental value for η(1760), the partial decay width to ωω is too small, which is not consistent with the BES result. If X(1835) is interpreted as $\eta(4\,^1S_0)$, the total decay width is compatible with the experimental data, and the main decay modes will be $\pi a_0(980)$ and $\pi a_0(1450)$, which needs to be checked experimentally. The assignment of X(2120) and X(2370) to $\eta'(3\,^1S_0)$ and $\eta'(4\,^1S_0)$ is disfavored in the present calculation because of the incompatibility of the decay widths.

Key words: X(1835), X(2120), X(2370), η(1760), chiral quark model, pseudoscalar meson

PACS: 12.39.Jh, 13.25.Jx, 14.40.Aq **DOI:** 10.1088/1674-1137/36/8/001

1 Introduction

In 2005, the BES Collaboration observed a narrow peak in the $\eta'\pi^+\pi^-$ invariant mass spectrum in the process $J/\psi\to\eta'\pi^+\pi^-$ with a statistic significance of 7.7σ. Fitting with the Breit-Wigner function yields mass and width [1]

$$M = 1833.7\pm6.1(\text{stat})\pm2.7(\text{syst})\ \text{MeV}/c^2$$

$$\Gamma = 67.7\pm20.3(\text{stat})\pm7.7(\text{syst})\ \text{MeV}/c^2,$$

and the product branching fraction

$$B(J/\psi\to\gamma X(1835))B(X(1835)\to\pi^+\pi^-\eta')$$

$$= (2.2\pm0.4(\text{stat})\pm0.4(\text{syst}))\times10^{-4}.$$

BES-III confirmed it in the same process with statistical significance larger than 20σ. The fitted mass and width are $M = 1836.5\pm3.0(\text{stat})^{+5.6}_{-2.1}(\text{syst})$ MeV/c^2, Γ=190 $\pm9(\text{stat})^{+38}_{-36}(\text{syst})$ MeV/c^2. Meanwhile, another two new resonances, X(2120) and X(2370), are also observed in the same process with the statistical significance larger than 7.2σ and 6.4σ, respectively. The fitted masses and decay widths are [2]

$$M = 2122.4\pm6.7(\text{stat})^{+4.7}_{-2.7}(\text{syst})\ \text{MeV}/c^2,$$

$$M = 2376.3\pm8.7(\text{stat})^{+3.2}_{-4.3}(\text{syst})\ \text{MeV}/c^2,$$

and

$$\Gamma = 83\pm16(\text{stat})^{+31}_{-17}(\text{syst})\ \text{MeV}/c^2,$$

$$\Gamma = 83\pm17(\text{stat})^{+44}_{-6}(\text{syst})\ \text{MeV}/c^2,$$

respectively. η(1760), whose nature is still controversial, was first reported by the Mark III Collaboration in the J/ψ radiative decays to ωω [3] and ρρ [4]. Then the DM2 Collaboration observed a large bump peaking at 1.77 GeV/c^2 in ωω invariant mass distribution in the process of $J/\psi\to\gamma\omega\omega$ ($\omega\to\pi^+\pi^-\pi^0$) [5] and the study of the decays $J/\psi\to\gamma\pi^+\pi^-\pi^+\pi^-$ and $J/\psi\to\gamma\pi^+\pi^-\pi^0\pi^0$ shows that both decays have a large ρρ dynamics [6]. The fitted mass and width are M = 1760±11 MeV and Γ = 60 ± 16 MeV. Recently, BES Collaboration reported its results on

Received 15 November 2011, Revised 18 January 2012
* Supported by National Natural Science Foundation of China (11035006, 11175088)
1) E-mail: jlping@njnu.edu.cn (corresponding author)

the decays $J/\psi \rightarrow \gamma\omega\omega$, $\omega \rightarrow \pi^+\pi^-\pi_0$ [7], the mass and width of the state turned out to be $M = 1744\pm10(\text{stat})\pm15$ MeV and $\Gamma=244^{+24}_{-21}\pm25$ MeV.

Much work has been devoted to the underlying structures of X(1835) and η(1760) [8]. For X(1835), the $p\bar{p}$ bound state is a plausible intepretation [9–12]. By calculating the mesonic decays of a baryonium resonance, Ding et al. claimed that the $p\bar{p}$ bound state favors the decay channel $X\rightarrow \eta4\pi$ over $X\rightarrow \eta3\pi$ [9]. In fact, it is just this work that stimulates the observation of the $J/\psi \rightarrow \eta'\pi^+\pi^-$ process in BES experiments. Using a semi-phenomenological potential model that can describe all the $N\bar{N}$ scattering data, Dedonder et al. found a broad spin-isospin singlet, the S-wave quasi-bound state of $N\bar{N}$, which can be used to explain the peak observed by BES [10]. Z. G. Wang et al. also calculated the mass of X(1835) as a baryonium in the framework of the QCD sum rule and the Bethe-Salpeter equation, and obtained consistent results with experimental data [11]. The large-N_c QCD was also applied to study the state X(1835) as a baryonium [12]. Interpretation of X(1835) as a glueball or a glueball mixed with pseudoscalar meson or baryonium is also proposed using the QCD sum rule [13–16]. Apart from these explanations for X(1835) as an exotic state, the conventional $q\bar{q}$ picture of X(1835) is also proposed. Huang and Zhu studied the behavior of X(1835) and thought that it could be taken as the second radial excitation of η′(958), in the effective Lagrangian approach [17]. The two-body decays of X(1835) as a $3\,^1S_0$ meson were also calculated by the quark-pair creation ($^3P_0$) model [18]. The results showed that the decay width was sensitive to the mixing angle of two states $X_n = (u\bar{u}+d\bar{d})/\sqrt{2}$ and $X_s = s\bar{s}$. Recently J. Yu et al. systematically studied the two-body strong decays and double pion decays of the η-family and assigned the X(1835) to the second radial excitation of η′(958), X(2120) and X(2370) to the third and fourth radial excitation of η(548)/η′(958), respectively [19]. For η(1760), J. Vijande et al. assigned it to be a $2\,^1S_0$ state of $s\bar{s}$ in the chiral quark model [20]. The assignment of η(1760) to the second radial excitation of η(548) was also proposed by J. S. Yu et al. [19]. Li and Page suggested that it could be a gluonic meson [21]. A glueball mixed with $q\bar{q}$ picture of η(1760) was also suggested by N. Wu et al. [22]. Stimulated by these experimental and theoretical works, we shall study whether η(1760), X(1835), X(2120) and X(2370) can be described in the simplest system-$q\bar{q}$ system.

In this work, the pseudoscalar meson spectrum is determined by the chiral quark model. The mixing angle between X_n and X_s is fixed through the system dynamics. Based on the mass spectra of η and η′, the possible candidates of X(1835), X(2120), X(2370) and η(1760) are assigned. Then the strong decay widths of the states are calculated in the framework of $^3P_0$ model, and to see the assignment is reasonable or not by comparing it with experimental data. The paper is organized as follows: a brief review of the $^3P_0$ model is given in Section 2. The chiral quark model is introduced and the meson spectrum and the wave functions of the mesons are obtained in Section 3. The numerical result of the strong decay is shown in Section 4. The last section is a summary.

2 The $^3P_0$ model of meson decay

The $^3P_0$ model, also known as the quark-pair creation (QPC) model, applied to the decay of meson A to meson B+C, was first proposed by Micu [23], and then developed by Le Yaouanc, Ackleh, Roberts et al. [24–26]. The $^3P_0$ model assumes that there is a quark and antiquark pair created in vacuum, the quantum number of the pair is $J^{PC} = 0^{++}$. Since vacuum is colorless and flavorless, the color and flavor singlet should be satisfied. The created pair is recombined with the quark-antiquark pair in initial meson and forms two mesons in the final state in two possible ways, which are shown in Fig. 1.

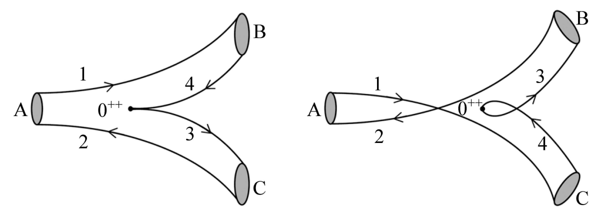

Fig. 1. The two possible diagrams contributing to $A\rightarrow B+C$ in the $^3P_0$ model.

In the non-relativistic limit, the transition operator T takes the form

$$T = -3\,\gamma\sum_m \langle 1m1-m|00\rangle \int \mathrm{d}\boldsymbol{p}_3\mathrm{d}\boldsymbol{p}_4\delta^3(\boldsymbol{p}_3+\boldsymbol{p}_4) \times\mathcal{Y}_1^m\left(\frac{\boldsymbol{p}_3-\boldsymbol{p}_4}{2}\right)\chi^{34}_{1-m}\phi^{34}_0\omega^{34}_0 b^\dagger_3(\boldsymbol{p}_3)d^\dagger_4(\boldsymbol{p}_4), \quad (1)$$

where the dimensionless parameter γ represents the strength of the quark-antiquark pair creation from vacuum and can be obtained by fitting the experimental data. $\boldsymbol{p}_3$ and $\boldsymbol{p}_4$ denote the momenta of the created quark and antiquark respectively. $\mathcal{Y}_l^m(\boldsymbol{p}) = |p|^l Y_l^m(\theta_p,\phi_p)$ is the l-th solid harmonic polynomial that gives the momentum-space distribution of the created quark-antiquark pair. χ^{34}_{1-m} reflects the triplet state of spin. $\phi^{34}_0=(u\bar{u}+d\bar{d}+s\bar{s})/\sqrt{3}$ and $\omega^{34}_0=(r\bar{r}+g\bar{g}+b\bar{b})/\sqrt{3}$ correspond to the flavor and color singlets, respectively. $b^\dagger_3(\boldsymbol{p}_3)$, $d^\dagger_4(\boldsymbol{p}_4)$ are the creation operators of the quark and antiquark, respectively.

To depict the meson state, we define

$$\begin{aligned}&|A(n_{\rm A}^{2S_{\rm A}+1}L_{{\rm A}\ J_{\rm A}M_{J_{\rm A}}})(\boldsymbol{P}_{\rm A})\rangle\\ \equiv&\ \sqrt{2E_{\rm A}}\sum_{M_{L_A},M_{S_{\rm A}}}\langle L_{\rm A}M_{L_{\rm A}}S_{\rm A}M_{S_{\rm A}}|J_{\rm A}M_{J_{\rm A}}\rangle\\ &\times\int{\rm d}\boldsymbol{p}_{\rm A}\chi^{12}_{S_{\rm A}M_{S_{\rm A}}}\phi^{12}_{\rm A}\omega^{12}_{\rm A}\left|q_1\left(\frac{m1}{m1+m2}\boldsymbol{P}_{\rm A}+p_{\rm A}\right)\right.\\ &\times\bar{q}_2\left.\left(\frac{m2}{m1+m2}\boldsymbol{P}_{\rm A}+p_{\rm A}\right)\right\rangle, \qquad (2)\end{aligned}$$

and the wave function is normalized as

$$\begin{aligned}&\left\langle A(n_{\rm A}^{2S_{\rm A}+1}L_{{\rm A}\ J_{\rm A}M_{J_{\rm A}}})(\boldsymbol{P}_{\rm A})\right|\\ &\times A(n_{\rm A}^{2S_{\rm A}+1}L_{{\rm A}\ J_{\rm A}M_{J_{\rm A}}})(\boldsymbol{P}'_{\rm A})\Big\rangle=2E_{\rm A}\delta^3(\boldsymbol{P}_{\rm A}-\boldsymbol{P}'_{\rm A}), \quad (3)\end{aligned}$$

where $\chi^{12}_{S_{\rm A}M_{S_{\rm A}}},\phi^{12}_{\rm A},\omega^{12}_{\rm A}$ represent the spin, flavor and color wave functions, respectively; $\boldsymbol{P}_{\rm A}$ is the center of mass momentum of meson A, and $\boldsymbol{p}_{\rm A}=(m_2\boldsymbol{p}_1-m_1\boldsymbol{p}_2)/(m_1+m_2)$ is the relative momentum of $q\bar{q}$ pair; $n_{\rm A}$ is the radial quantum number; $|L_{\rm A},M_{L_{\rm A}}\rangle,|S_{\rm A},M_{S_{\rm A}}\rangle,|J_{\rm A},M_{J_{\rm A}}\rangle$ are the quantum number of orbit angular momentum between $q\bar{q}$ pair in meson A, the total spin and the total angular momentum of the pair, respectively; $\langle L_{\rm A}M_{L_{\rm A}}S_{\rm A}M_{S_{\rm A}}|J_{\rm A}M_{J_{\rm A}}\rangle$ denotes a Clebsch-Gordan coefficient, $E_{\rm A}$ is the total energy of the meson A.

The S-matrix describing a strong decay process of $\rm A\to B+C$ is written as

$$\langle BC|S|A\rangle=I-2\pi{\rm i}\delta(E_{\rm A}-E_{\rm B}-E_{\rm C})\langle BC|T|A\rangle, \quad (4)$$

and

$$\langle BC|T|A\rangle=\delta^3(\boldsymbol{P}_{\rm A}-\boldsymbol{P}_{\rm B}-\boldsymbol{P}_{\rm C})\mathcal{M}^{M_{J_{\rm A}}M_{J_{\rm B}}M_{J_{\rm C}}}, \quad (5)$$

where $\mathcal{M}^{M_{J_{\rm A}}M_{J_{\rm B}}M_{J_{\rm C}}}$ is the helicity amplitude of $\rm A\to B+C$. Taking the center of the mass frame of meson A: $\boldsymbol{P}_{\rm A}=0$, one can obtain $\mathcal{M}^{M_{J_{\rm A}}M_{J_{\rm B}}M_{J_{\rm C}}}$ for the decay process in terms of overlap integrals,

$$\begin{aligned}\mathcal{M}^{M_{J_{\rm A}}M_{J_{\rm B}}M_{J_{\rm C}}}=&\ 3\gamma\sum_{\{M\}}\langle L_{\rm A}M_{L_{\rm A}}S_{\rm A}M_{S_{\rm A}}|J_{\rm A}M_{J_{\rm A}}\rangle\langle L_{\rm B}M_{L_{\rm B}}S_{\rm B}M_{S_{\rm B}}|J_{\rm B}M_{J_{\rm B}}\rangle\langle L_{\rm C}M_{L_{\rm C}}S_{\rm C}M_{S_{\rm C}}|J_{\rm C}M_{J_{\rm C}}\rangle\\ &\times\langle 1m1-m|00\rangle\langle\chi^{14}_{S_{\rm B}M_{S_{\rm B}}}\chi^{32}_{S_{\rm C}M_{S_{\rm C}}}|\chi^{12}_{S_{\rm A}M_{S_{\rm A}}}\chi^{34}_{1-m}\rangle[\langle\omega^{14}_{\rm B}\omega^{32}_{\rm C}|\omega^{12}_{\rm A}\omega^{34}_0\rangle\langle\phi^{14}_{\rm B}\phi^{32}_{\rm C}|\phi^{12}_{\rm A}\phi^{34}_0\rangle\\ &\times\mathcal{I}^{M_{L_{\rm A}},m}_{M_{L_{\rm B}},M_{L_{\rm C}}}(\boldsymbol{P},m_1,m_2,m_3)+(-1)^{1+S_{\rm A}+S_{\rm B}+S_{\rm C}}\langle\omega^{32}_{\rm B}\omega^{14}_{\rm C}|\omega^{12}_{\rm A}\omega^{34}_0\rangle\langle\phi^{32}_{\rm B}\phi^{14}_{\rm C}|\phi^{12}_{\rm A}\phi^{34}_0\rangle\\ &\times\mathcal{I}^{M_{L_{\rm A}},m}_{M_{L_{\rm B}},M_{L_{\rm C}}}(-\boldsymbol{P},m_2,m_1,m_3)], \qquad (6)\end{aligned}$$

where $\{M\}=M_{L_{\rm A}},M_{S_{\rm A}},M_{L_{\rm B}},M_{S_{\rm B}},M_{L_{\rm C}},M_{S_{\rm C}},m$, the momentum space integral $\mathcal{I}^{M_{L_{\rm A}},m}_{M_{L_{\rm B}},M_{L_{\rm C}}}(\boldsymbol{P},m_1,m_2,m_3)$ and $\mathcal{I}^{M_{L_{\rm A}},m}_{M_{L_{\rm B}},M_{L_{\rm C}}}(-\boldsymbol{P},m_1,m_2,m_3)$ are given by

$$\begin{aligned}\mathcal{I}^{M_{L_{\rm A}},m}_{M_{L_{\rm B}},M_{L_{\rm C}}}(\boldsymbol{P},m_1,m_2,m_3)=&\ \sqrt{8E_{\rm A}E_{\rm B}E_{\rm C}}\int{\rm d}\boldsymbol{p}\,\psi^*_{n_{\rm B}L_{\rm B}M_{L_{\rm B}}}\left(\frac{m_3}{m_1+m_3}\boldsymbol{P}+\boldsymbol{p}\right)\psi^*_{n_{\rm C}L_{\rm C}M_{L_{\rm C}}}\left(\frac{m_3}{m_2+m_3}\boldsymbol{P}+\boldsymbol{p}\right)\\ &\times\psi_{n_{\rm A}L_{\rm A}M_{L_{\rm A}}}(\boldsymbol{P}+\boldsymbol{p})\mathcal{Y}^m_1(\boldsymbol{p}), \qquad (7)\end{aligned}$$

$$\begin{aligned}\mathcal{I}^{M_{L_{\rm A}},m}_{M_{L_{\rm B}},M_{L_{\rm C}}}(-\boldsymbol{P},m_1,m_2,m_3)=&\ \sqrt{8E_{\rm A}E_{\rm B}E_{\rm C}}\int{\rm d}\boldsymbol{p}\,\psi^*_{n_{\rm B}L_{\rm B}M_{L_{\rm B}}}\left(-\frac{m_3}{m_1+m_3}\boldsymbol{P}+\boldsymbol{p}\right)\psi^*_{n_{\rm C}L_{\rm C}M_{L_{\rm C}}}\left(-\frac{m_3}{m_2+m_3}\boldsymbol{P}+\boldsymbol{p}\right)\\ &\times\psi_{n_{\rm A}L_{\rm A}M_{L_{\rm A}}}(-\boldsymbol{P}+\boldsymbol{p})\mathcal{Y}^m_1(\boldsymbol{p}), \qquad (8)\end{aligned}$$

where $\boldsymbol{P}_{\rm B}=-\boldsymbol{P}_{\rm C}=\boldsymbol{P},\boldsymbol{p}=\boldsymbol{p}_3$, and m_3 is the mass of the created quark. The spacial wavefunction is taken as the simple harmonic oscillator (SHO) wavefunction. In momentum space, the SHO wavefunction reads

$$\varPsi_{nLM_L}(\boldsymbol{p})=(-1)^n(-{\rm i})^LR^{L+\frac{3}{2}}\sqrt{\frac{2n!}{\varGamma\left(n+L+\dfrac{3}{2}\right)}}\times\exp\left(-\frac{R^2p^2}{2}\right)L_n^{L+\frac{1}{2}}(R^2p^2)\mathcal{Y}^{M_L}_L(\boldsymbol{p}), \qquad (9)$$

where $\mathcal{Y}_L^{M_L}(\boldsymbol{p})$ is the solid harmonic polynomial; R is the parameter of the SHO wavefunction; $\boldsymbol{p}$ is the relative momentum between $q\bar{q}$ pair within a meson; $L_n^{L+\frac{1}{2}}(R^2p^2)$ is the associated Laguerre polynomial.

The decay width can be written as follows

$$\Gamma=\pi^2\frac{|\boldsymbol{P}|}{M_A^2(1+\delta_{BC})}\sum_{JL}\left|\mathcal{M}^{JL}\right|^2, \quad (10)$$

where $\mathcal{M}^{JL}$ is the partial wave amplitude, which is related to the helicity amplitude $\mathcal{M}^{M_{J_A}M_{J_B}M_{J_C}}$ via the Jacob-Wick formula [27]

$$\begin{aligned}\mathcal{M}^{JL}(A\to BC) &= \frac{\sqrt{2L+1}}{2J_A+1}\sum_{M_{J_B},M_{J_C}}\langle L0JM_{J_A}|J_AM_{J_A}\rangle \\ &\times\langle J_BM_{J_B}J_CM_{J_C}|JM_{J_A}\rangle \\ &\times\mathcal{M}^{M_{J_A}M_{J_B}M_{J_C}}(\boldsymbol{P}), \quad (11)\end{aligned}$$

where $\boldsymbol{J}=\boldsymbol{J}_B+\boldsymbol{J}_C$, $\boldsymbol{J}_A=\boldsymbol{J}_B+\boldsymbol{J}_C+\boldsymbol{L}$, $|\boldsymbol{P}|=|\boldsymbol{P}_B|=|\boldsymbol{P}_C|$. According to the calculation of 2-body phase space, one can get

$$|\boldsymbol{P}|=\frac{\sqrt{[M_A^2-(M_B+M_C)^2][M_A^2-(M_B-M_C)^2]}}{2M_A},$$

where M_A, M_B, and M_C are the masses of the mesons A, B, and C, respectively.

3 The masses of the mesons

To calculate the meson spectrum, a QCD-inspired model, constituent quark model, is used. The model incorporates the perturbative (one gluon exchange) and nonperturbative (color confinement and spontaneous breaking of chiral symmetry) properties of QCD. The constituent quark mass originates from the spontaneous breaking of chiral symmetry and consequently the constituent quarks should interact through the exchange of Goldstone bosons [28], in addition to the one-gluon-exchange. To describe the hadron-hadron interaction, the chiral partner of pions, the σ-meson, is also used. So the model Hamiltonian is

$$H = m_1+m_2+\frac{\boldsymbol{p}^2}{2\mu}+V^C+V^G+V^\chi+V^\sigma, \quad (12)$$

$$V^C = \boldsymbol{\lambda}_1^c\cdot\boldsymbol{\lambda}_2^c[-a_c(1-e^{-\mu_c r})+\Delta]+V_{SO}^C,$$

$$\begin{aligned}V_{SO}^C &= -\boldsymbol{\lambda}_1^c\cdot\boldsymbol{\lambda}_2^c\frac{a_c\mu_c e^{-\mu_c r}}{4m_1^2m_2^2r}[(m_1^2+m_2^2)(1-2a_s) \\ &\quad +4m_im_j(1-a_s)]\ \boldsymbol{S}\cdot\boldsymbol{L},\end{aligned}$$

$$V^G = V_C^G+V_{SO}^G+V_T^G,$$

$$V_C^G = \frac{\alpha_s}{4}\boldsymbol{\lambda}_1^c\cdot\boldsymbol{\lambda}_2^c\left\{\frac{1}{r}-\frac{\boldsymbol{\sigma}_1\cdot\boldsymbol{\sigma}_2}{6m_1m_2}\frac{e^{-r/r_0(\mu)}}{r\,r_0^2(\mu)}\right\},$$

$$\begin{aligned}V_{OGE}^{SO} &= -\frac{\alpha_s}{16}\frac{\boldsymbol{\lambda}_1^c\cdot\boldsymbol{\lambda}_2^c}{m_1^2m_2^2}\left[\frac{1}{r^3}-\frac{e^{-r/r_g(\mu)}}{r^3}\left(1+\frac{r}{r_g(\mu)}\right)\right] \\ &\quad\times[((m_1+m_2)^2+2m_1m_2)\boldsymbol{S}\cdot\boldsymbol{L}],\end{aligned}$$

$$\begin{aligned}V_{OGE}^T &= -\frac{1}{16}\frac{\alpha_s}{m_1m_2}\boldsymbol{\lambda}_1^c\cdot\boldsymbol{\lambda}_2^c\left[\frac{1}{r^3}-\frac{e^{-r/r_g(\mu)}}{r}\right. \\ &\quad\left.\times\left(\frac{1}{r^2}+\frac{1}{3r_g^2(\mu)}+\frac{1}{r\,r_g(\mu)}\right)\right]S_{12},\end{aligned}$$

$$\begin{aligned}V_\chi &= (v_\pi^C+v_\pi^T)\sum_{a=1}^{3}\lambda_1^a\ \lambda_2^a+(v_K^C+v_K^T)\sum_{a=4}^{7}\lambda_1^a\ \lambda_2^a \\ &\quad+(v_\eta^C+v_\eta^T)(\lambda_1^8\ \lambda_2^8\cos\theta_P-\lambda_1^0\ \lambda_2^0\sin\theta_P),\end{aligned}$$

$$v_\chi^C = C_1\left[Y(m_\chi r)-\frac{\Lambda_\chi^3}{m_\chi^3}Y(\Lambda_\chi r)\right]\boldsymbol{\sigma}_1\cdot\boldsymbol{\sigma}_2,$$

$$v_\chi^T = C_1\left[H(m_\chi r)-\frac{\Lambda_\chi^3}{m_\chi^3}H(\Lambda_\chi r)\right]S_{12},$$

$$C_1 = \frac{g_{ch}^2}{4\pi}\frac{m_\chi^2}{12m_1m_2}\frac{\Lambda_\chi^2}{\Lambda_\chi^2-m_\chi^2}m_\chi, \quad \chi=\pi,K,\eta,$$

$$V_\sigma = -C_2\left[Y(m_\sigma r)-\frac{\Lambda_\sigma}{m_\sigma}Y(\Lambda_\sigma r)\right]+V_\sigma^{SO},$$

$$V_\sigma^{SO} = -C_2\frac{m_\sigma^2}{2m_1m_2}\left[G(m_\sigma r)-\frac{\Lambda_\sigma^3}{m_\sigma^3}G(\Lambda_\sigma r)\right]\boldsymbol{S}\cdot\boldsymbol{L},$$

$$C_2 = \frac{g_{ch}^2}{4\pi}\frac{\Lambda_\sigma^2}{\Lambda_\sigma^2-m_\sigma^2}m_\sigma,$$

$$S_{12} = 3(\boldsymbol{\sigma}_1\cdot\hat{\boldsymbol{r}})(\boldsymbol{\sigma}_2\cdot\hat{\boldsymbol{r}})-\boldsymbol{\sigma}_1\cdot\boldsymbol{\sigma}_2,$$

$$Y(x) = \frac{e^{-x}}{x}, \quad H(x)=\left(1+\frac{3}{x}+\frac{3}{x^2}\right)Y(x),$$

$$G(x) = \left(1+\frac{1}{x}\right)\frac{Y(x)}{x},$$

where $r=|\boldsymbol{r}_1-\boldsymbol{r}_2|$ and $\boldsymbol{p}=(\boldsymbol{p}_1-\boldsymbol{p}_2)/2$, $r_0(\mu)=\hat{r}_0/\mu$, $r_g(\mu)=\hat{r}_g/\mu$. Other symbols have their usual meanings. The effective running coupling constant is given by

$$\alpha_s(\mu)=\frac{\alpha_0}{\ln\left(\frac{\mu^2+\mu_0^2}{\Lambda_0^2}\right)}, \quad (13)$$

where μ is the reduced mass of the $q\bar{q}$ system. The chiral coupling constant g_{ch} is determined from the πNN coupling constant through

$$\frac{g_{\rm ch}^2}{4\pi}=\left(\frac{3}{5}\right)^2\frac{g_{\pi\rm NN}^2}{4\pi}\frac{m_{\rm u,d}^2}{m_{\rm N}^2}. \tag{14}$$

The meson spectrum is obtained by solving the Schrödinger equation,

$$H\Psi = E\Psi, \tag{15}$$

$$\Psi = [\psi_{nLM_L}\chi_{\rm SM_S}]_{JM_J}\chi_{\rm c}\chi_{\rm f}, \tag{16}$$

where $\chi_{\rm SM_S}$, $\chi_{\rm c}$, $\chi_{\rm f}$ are the spin, color and flavor wavefunctions of the meson, respectively, and can be constructed through the symmetry. The spacial wavefunction $\psi_{nLM_L} = R_{nL}(r)Y_{LM_L}(\Omega)$ is obtained by solving the second-order differential equation. The efficient numerical method, i.e., the Numerov method [29], is used here. The model parameters, which are listed in Table 1, are fixed by fitting the experimental data of the meson spectrum. Parts of the obtained meson spectrum are shown in Tables 2 and 3. The detailed results can be found in Ref. [20]. To calculate the strong decay of mesons analytically in the $^3P_0$ model, the obtained radial part of the spacial wavefunction $R_{nL}(r)$ is fitted by the SHO,

$$R_{nL}(r) = \beta^{(L+\frac{3}{2})}\sqrt{\frac{2n!}{\Gamma\left(n+L+\frac{3}{2}\right)}}\exp\left(-\frac{\beta^2r^2}{2}\right) \times r^L L_n^{L+\frac{1}{2}}(\beta^2r^2). \tag{17}$$

The fitted values of parameter β are also listed in Tables 2 and 3.

Table 1. Model parameters. The masses of mesons π, K, η take the experimental values.

$m_{\rm u,d}$/ MeV	$m_{\rm s}$/ MeV	$a_{\rm c}$/ MeV	$\mu_{\rm c}$/ fm^{-1}	Δ/ MeV	$a_{\rm s}$ —
313	555	430	0.7	181.10	0.777
α_0 —	Λ_0/ fm^{-1}	μ_0/ MeV	$\hat{r}_0$/ (MeV·fm)	$\hat{r}_{\rm g}$/ (MeV·fm)	
2.118	0.113	36.976	28.170	34.500	
Λ_π/ fm^{-1}	Λ_σ/ fm^{-1}	$\Lambda_{\rm K}$/ fm^{-1}	Λ_η/ fm^{-1}	$g_{\rm ch}^2/4\pi$ —	$\theta_{\rm P}$/ (°)
4.20	4.20	5.20	5.20	0.54	−15

There are two types of $I=0$ states. One is composed of u, d-quark and ū, d̄-antiquark, another is composed of the s-quark and the s̄-antiquark. They are mixed in the flavor $SU(3)$ symmetry to form flavor singlet η_1 and octet η_8. However, flavor $SU(3)$ is broken. In experiments, we have η and η′ instead of η_1 and η_8 for the pseudoscalar. In the present calculation, flavor $SU(3)$ symmetry is not used, so we have $I=0$ flavor wavefunctions $X_{\rm n}$ and $X_{\rm s}$. As a consequence of K-meson exchange, they are mixed. To obtain the masses of the $I=0$ states, the following procedure is taken. First, the Schrödinger equation for $X_{\rm n}$ and $X_{\rm s}$ are solved separately (K-meson exchange is not employed). Secondly, by using the wavefunctions $\Psi_{\rm n}$ and $\Psi_{\rm s}$ obtained in the first step and taking into account the K-meson exchange, the eigenenergies and eigenstates can be obtained by diagonalizing the Hamiltonian matrix

$$\begin{pmatrix} H_{\rm nn} & H_{\rm ns} \\ H_{\rm sn} & H_{\rm ss}\end{pmatrix}\begin{pmatrix} C_{\rm n} \\ C_{\rm s}\end{pmatrix}=E\begin{pmatrix} C_{\rm n} \\ C_{\rm s}\end{pmatrix}, \tag{18}$$

where $H_{\rm nn} = \langle\Psi_{\rm n}|H|\Psi_{\rm n}\rangle$, $H_{\rm ns} = \langle\Psi_{\rm n}|V_{\rm K}|\Psi_{\rm s}\rangle = H_{\rm sn}$ and $H_{\rm ss} = \langle\Psi_{\rm s}|H|\Psi_{\rm s}\rangle$. The eigen-state is $|\Psi\rangle = C_{\rm n}|\Psi_{\rm n}\rangle + C_{\rm s}|\Psi_{\rm s}\rangle$. The obtained eigenenergies and eigenstates are shown in Table 3. From Table 3, one finds that η(1760), X(1835), X(2120), X(2370) may be interpreted as $\eta'(2^1S_0)$, $\eta(4^1S_0)$, $\eta'(3^1S_0)$ and $\eta'(4^1S_0)$, respectively, by comparing the theoretical masses with the experimental data. To check these assignments, the decay properties of the states should be calculated, which is discussed in the next section.

Table 2. The mass of $I=1, \frac{1}{2}$ mesons and the values of fitted β.

$n^{2S+1}L_J$	states	isospin	mass/ MeV	β/ fm^{-1}	R/ GeV^{-1}
1^1S_0	π	1	139	2.308	2.196
2^1S_0	π(1300)	1	1288	1.434	3.534
1^3S_1	ρ	1	772	1.438	3.522
2^3S_1	ρ(1450)	1	1478	1.096	4.624
1^1P_1	$b_1(1235)$	1	1234	1.243	4.077
1^3P_0	$a_0(980)$	1	984	1.473	3.440
2^3P_0	$a_0(1450)$	1	1587	1.125	4.505
1^3P_1	$a_1(1260)$	1	1205	1.300	3.898
1^3P_2	$a_2(1320)$	1	1327	1.106	4.582
1^3P_2	$a_2(1700)$	1	1732	0.890	5.694
1^1S_0	K	1/2	496	2.313	2.191
2^1S_0	K(1460)	1/2	1472	1.545	3.280
1^3S_1	K*(892)	1/2	910	1.629	3.111
2^3S_1	K(1630)	1/2	1620	1.262	4.016
1^1P_1	$K_1(1400)$	1/2	1414	1.371	3.696
1^3P_0	$K_0^*(1430)$	1/2	1213	1.572	3.224
2^3P_0	$K_0^*(1950)$	1/2	1768	1.243	4.077
1^3P_1	$K_1(273)$	1/2	1352	1.435	3.531
1^3P_2	$K_2^*(1430)$	1/2	1450	1.572	3.224
1^3D_1	$K_1(1680)$	1/2	1698	1.205	4.206

Table 3. The masses of $I=0$ mesons and the value of fitted β ($\beta=C_n^2\beta_n+C_s^2\beta_s$).

$(nL)J^{PC}$	states	mass/MeV	C_n	C_s	β/fm^{-1}	R/GeV^{-1}
$1\,^1S_0$	η	572	8.6564×10^{-1}	-5.0066×10^{-1}	1.732693	2.924
$1\,^1S_0$	η′(958)	956	5.0066×10^{-1}	8.6564×10^{-1}	2.064307	2.455
$2\,^1S_0$	η(1295)	1290	9.6360×10^{-1}	-2.67323×10^{-1}	1.183–1.666	3.041–4.284
$2\,^1S_0$	η′(1760)	1795	2.6732×10^{-1}	9.6360×10^{-1}	1.183–1.666	3.041–4.284
$3\,^1S_0$	η(3S)	1563	9.9350×10^{-1}	-1.1380×10^{-1}	0.929–1.360	3.726–5.455
$3\,^1S_0$	η′(3S)	2276	1.1380×10^{-1}	9.9350×10^{-1}	0.929–1.360	3.726–5.455
$4\,^1S_0$	η(4S)	1807	9.9935×10^{-1}	-3.5928×10^{-2}	0.6725–1.0995	4.607–7.530
$4\,^1S_0$	η′(4S)	2390	3.5928×10^{-2}	9.9935×10^{-1}	0.6725–1.0995	4.607–7.530
$1\,^3S_1$	ω(782)	691	9.9499×10^{-1}	9.9967×10^{-2}	1.547	3.276
$1\,^3S_1$	ϕ(1020)	1020	-9.9967×10^{-2}	9.9499×10^{-1}	1.918	2.642
$2\,^3S_1$	ω(1420)	1444	9.9852×10^{-1}	5.4331×10^{-2}	1.163	4.357
$2\,^3S_1$	ϕ(1680)	1726	-5.4331×10^{-2}	9.9852×10^{-1}	1.506	3.365
$1\,^1P_1$	h_1(1170)	1257	1.0	0	1.202	4.216
$1\,^1P_1$	h_1'	1511	0	1.0	1.581	3.205
$1\,^3P_2$	f_2(1270)	1311	1.0	0	1.112	4.557
$1\,^3P_2$	f_2'(1525)	1556	0	1.0	1.496	3.387

4 The strong decay of the candidates for η(1760), X(1835), X(2120), X(2370)

η, η′ and their radial excitations have the same quantum numbers $IJ^{PC}=00^{-+}$. According to the $^3P_0$ model discussed above, the isospins of mesons B and C can take the values $I=0,1/2$, or 1 with the condition $\boldsymbol{I}_B+\boldsymbol{I}_C=\boldsymbol{I}_A$. All the allowed two-body decay modes of η(η′) family and corresponding partial-wave amplitudes are listed in Table 4.

To calculate the strong decay widths of mesons, the strength of the quark-antiquark pair creation from the vacuum, γ, has to be fixed. It is obtained by fitting the experimental values of the strong decay widths of light and charmed mesons, charmonium, and baryons. In the present work, for the non-strange quark pair creation, $\gamma=6.95$, and for $s\bar{s}$ creation, $\gamma_s=\gamma/3$, which are adopted in many researches [30–33].

4.1 η($2\,^1S_0$) and η′($2\,^1S_0$)

From the mass of state η($2\,^1S_0$), it is natural to assign the state η(1295) to it. In Fig. 2, the dependence of the partial widths of the strong decay of η($2\,^1S_0$) on R_A is shown. Taking R_A=3.0–4.3 GeV^{-1} discussed above, the total width ranges from 16 to 35 MeV, which is a little lower than the experimental value of the total width $\Gamma=55\pm5$ MeV [34]. The assignment is reasonable because the three-body decay widths have not been taken into account in the present work.

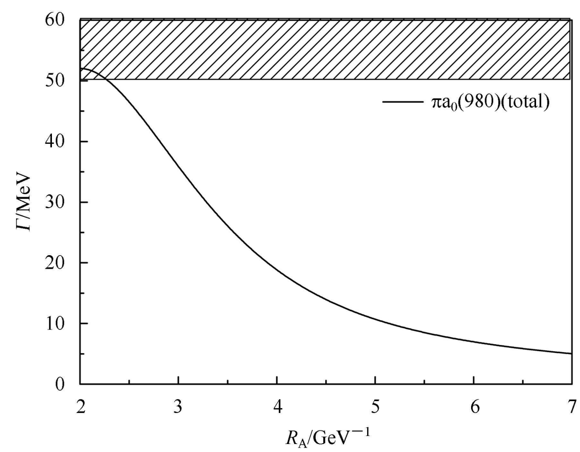

Fig. 2. The strong decay width of the η($2\,^1S_0$).

The experimental evidence for η(1760) is controversial. There are large differences between the observations of the MARK III, DM2 and BES collaborations [1, 3–6]. In our calculation, the mass of η′(2^1S_1) is 1795 MeV, which is close to the experimental mass of η(1760). So it can be taken as a candidate of η(1760). In Fig. 3, we show the dependence of the partial widths of the strong decay of the η′($2\,^1S_0$) on the R_A. Taking R_A =3.0–4.3 GeV^{-1} discussed above, the total width ranges from 256 to 404 MeV, which is much larger than the results given by Mark III and the DM2 Collaboration, but falls within the range of the BES experimental data. In this range, η′($2\,^1S_0$) has a sizable branching ration into πa$_0$(980), πa$_2$(1320), ρρ, and KK*, but the partial width to ωω is rather small. So the assignment of η(1760) to η′($2\,^1S_0$) is disfavored in the present calculation. In Ref. [19], η(1760) is taken as η(3S), the total decay width is between

Table 4. The allowed decay modes and the amplitudes of the radial excited states of η and η′. For $X_{\rm n}$ decay, $\phi_{\rm f}=\sqrt{\frac{1}{2}},\ \sqrt{\frac{1}{3}},\ \sqrt{\frac{1}{6}},\ 0$ for $I_{\rm B}=I_{\rm C}=1,\ 1/2,\ 0({\rm X_n}),\ 0({\rm X_s})$ and for $X_{\rm s}$ decay, $\phi_{\rm f}=0,\ \sqrt{\frac{2}{3}},\ 0,\ \sqrt{\frac{1}{3}}$ for $I_{\rm B}=I_{\rm C}=1,\ 1/2,\ 0(X_{\rm n}),\ 0(X_{\rm s})$.

$X\to {}^1S_0+{}^3P_0$	$\pi a_0(980),\ \pi a_0(1450),\ \pi(1300)a_0(980),$	$M^{JL}=M^{00}=M^{000}$
	$KK_0^*(1430),\ KK_0^*(1950)$	$M^{000}=\sqrt{\frac{1}{36}}(I^{-1,-1}_{0,0}+I^{0,0}_{0,0}+I^{1,1}_{0,0})\phi_{\rm f}$
$X\to {}^1S_0+{}^3P_2$	$\pi a_2(1320),\ \pi a_2(1700),\ KK_2^*(1430),\ \eta f_2(1270),$	$M^{JL}=M^{22}=M^{000}$
	$\eta' f_2(1270),\ \eta f_2'(1525)$	$M^{000}=\sqrt{\frac{1}{72}}(I^{-1,-1}_{0,0}-2M^{0,0}_{0,0}+M^{1,1}_{0,0})\phi_{\rm f}$
$X\to {}^1S_0+{}^3S_1$	$KK^*,\ KK^*(1410),\ K(1460)K^*$	$M^{JL}=M^{11}=-M^{000}$
		$M^{000}=-\sqrt{\frac{1}{12}}I^{0,0}_{0,0}\phi_{\rm f}$
$X\to {}^1S_0+{}^3D_1$	$KK^*(1680)$	$M^{JL}=M^{11}=-M^{000}$
		$M^{000}=\left(\sqrt{\frac{1}{40}}I^{-1,-1}_{0,0}+\sqrt{\frac{1}{30}}I^{0,0}_{0,0}+\sqrt{\frac{1}{40}}I^{1,1}_{0,0}\right)\phi_{\rm f}$
$X\to {}^3S_1+{}^3P_1$	$\rho a_1(1640),\ \rho a_1(1260),\ K^*K_1(1273),\ \omega f_1(1285)$	$M^{JL}=M^{00}+M^{22}$
		$M^{00}=\sqrt{\frac{1}{3}}(M^{0-11}-M^{000}+M^{01-1})$
		$M^{22}=\sqrt{\frac{1}{6}}(M^{0-11}+2M^{000}+M^{01-1})$
		$M^{0-11}=-\sqrt{\frac{1}{24}}(I^{0,0}_{0,0}+I^{1,1}_{0,0})\phi_{\rm f}$
		$M^{000}=\sqrt{\frac{1}{24}}(I^{-1,-1}_{0,0}+I^{1,1}_{0,0})\phi_{\rm f}$
		$M^{01-1}=-\sqrt{\frac{1}{24}}(I^{0,0}_{0,0}+I^{1,1}_{0,0})\phi_{\rm f}$
$X\to {}^3S_1+{}^3S_1$	$\rho\rho,\ \rho\rho(1450),\ \omega\omega,\ \omega\omega(1420),$	$M^{JL}=M^{11}=\sqrt{\frac{1}{2}}(M^{0-11}-M^{01-1})$
	$K^*K^*,\ K^*K^*(1410),\ \phi\phi$	$M^{0-11}=\sqrt{\frac{1}{12}}(I^{0,0}_{0,0})\phi_{\rm f},\ M^{0-11}=-\sqrt{\frac{1}{12}}(I^{0,0}_{0,0})\phi_{\rm f}$
$X\to {}^3S_1+{}^1P_1$	$\rho b_1(1235),\ K^*K_1(1400),\ \omega h_1(1170)$	$M^{JL}=M^{00}+M^{22}$
		$M^{00}=\sqrt{\frac{1}{3}}(M^{0-11}-M^{000}+M^{01-1})$
		$M^{22}=\sqrt{\frac{1}{6}}(M^{0-11}+2M^{000}+M^{01-1})$
		$M^{0-11}=\sqrt{\frac{1}{12}}I^{1,1}_{0,0}\phi_{\rm f},\quad M^{000}=-\sqrt{\frac{1}{12}}I^{1,1}_{0,0}\phi_{\rm f}$
		$M^{01-1}=\sqrt{\frac{1}{12}}I^{-1,-1}_{0,0}\phi_{\rm f}$
$X\to {}^3S_1+{}^3P_2$	$\rho a_2(1320),\ K^*K_2^*(1430)$	$M^{JL}=M^{22}=-\sqrt{\frac{1}{2}}(M^{0-11}-M^{01-1})$
		$M^{0-11}=\sqrt{\frac{1}{24}}(I^{0,0}_{0,0}-I^{1,1}_{0,0})\phi_{\rm f}$
		$M^{01-1}=\sqrt{\frac{1}{24}}(I^{-1,-1}_{0,0}-I^{1,1}_{0,0})\phi_{\rm f}$

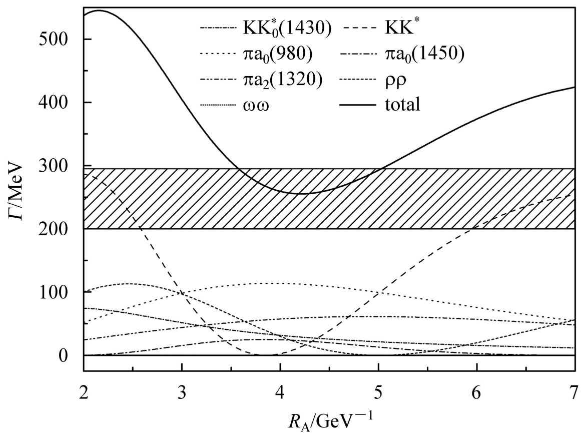

Fig. 3. The strong decay widths of the $\eta'(2\,^1S_0)$.

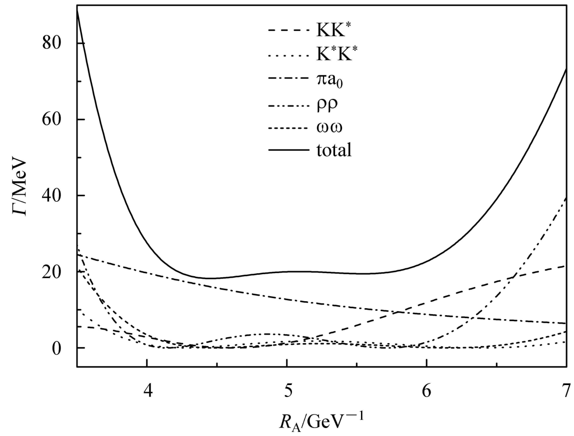

Fig. 4. The strong decay widths of the $\eta(3\,^1S_0)$.

60–100 MeV, which falls in the range of DM2's results, but is far below the BES's results.

4.2 $\eta(3\,^1S_0)$ and $\eta'(3\,^1S_0)$

The calculated mass of $\eta(3\,^1S_0)$ is 1563 MeV, which is rather higher than the mass of the observed state $\eta(1475)$. The strong decay width of $\eta(3\,^1S_0)$ is shown in Fig. 4. Compared with the experimental total width of $\eta(1475)$, $\Gamma=85\pm9$ MeV (the dominated decay process is $K\bar{K}\pi$), the assignment of $\eta(1475)$ to $\eta(3\,^1S_0)$ is possible. However, because of the large mass difference, further study is needed.

Besides confirming the existence of X(1835) in the $\pi^+\pi^-\eta'$ invariant-mass spectrum in the process $J/\psi\rightarrow\eta'\pi^+\pi^-$, another two states X(2120) and X(2370) are observed by BESIII with statistical significance larger than 7.2σ and 6.4σ, respectively. By comparing the masses of the $\eta(\eta')$ family, it is possible to take $\eta'(3\,^1S_0)$ as the candidates of X(2120). Because of its large mass, many strong decay modes are allowed. Because both X_n and X_s have contributions to the state $n\bar{s}s\bar{n}$, the partial width of the strong decay to two isospin $I=\dfrac{1}{2}$ mesons is generally much larger than that to two isospin 1 or 0 mesons. So the

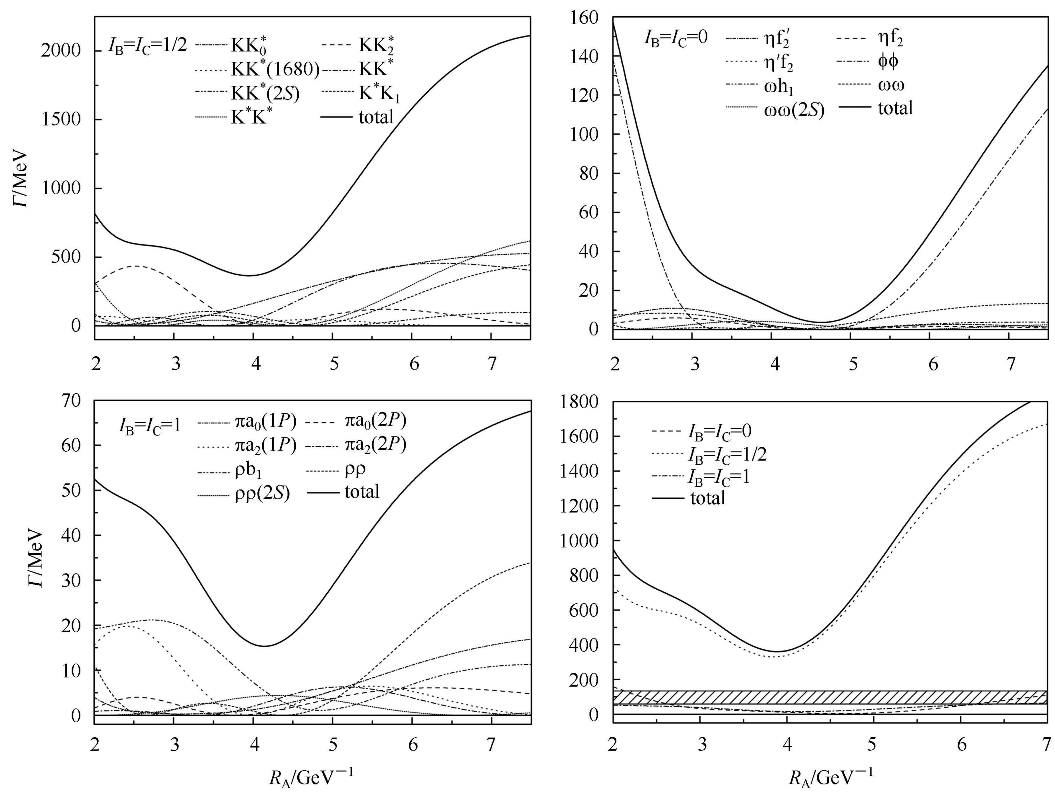

Fig. 5. The strong decay widths of the $\eta'(3\,^1S_0)$.

main decay channels of $\eta'(3\,^1S_0)$ are KK_0^* and KK^*. In Fig. 5, the partial widths of their strong decays are shown. For $\eta'(3\,^1S_0)$ with R_A=3.7–5.6 GeV^{-1}, the decay widths are much higher than the experimental value from BESIII. So the assignment of X(2120) to $\eta'(3\,^1S_0)$ is disfavored. In fact, the calculated mass of $\eta'(3\,^1S_0)$ is more close to the observed state η(2225) with mass and width, 2226 ± 16 MeV and $\Gamma=185^{+70}_{-40}$ MeV. The calculated width is at least 2 times the width of η(2225). Considering the uncertainty of the $^3P_0$ model, the assignment cannot be excluded.

4.3 $\eta(4\,^1S_0)$ and $\eta'(4\,^1S_0)$

In the present calculation, the mass of $\eta(4\,^1S_0)$, 1807 MeV, is close to the mass of X(1835), so the assignment of X(1835) to $\eta(4\,^1S_0)$ is possible, which is different from the assignment of Ref. [19], $\eta'(3S)$. In Fig. 6, the dependence of the partial widths of the strong decay of the $\eta(4\,^1S_0)$ on the R_A is shown. From the mass calculation, R_A=4.6–7.5 GeV^{-1} is obtained. In this range, the total width ranges from 54 to 692 MeV, which falls within the range of the BES experimental data, and the main decay modes are $\pi a_0(980)$ and $\pi a_0(1450)$. We strongly suggest an experimental search for X(1835) in these modes to justify the $\eta(4\,^1S_0)$ assignment.

The calculated mass of $\eta'(4\,^1S_0)$ is 2390 MeV, which is close to the mass of X(2370), so the possible candidate of X(2370) is $\eta'(4\,^1S_0)$. The partial decay widths of $\eta'(4\,^1S_0)$ are shown in Fig. 7. For $\eta'(4\,^1S_0)$ with R_A =4.6–7.5 GeV^{-1}, the main decay channels of $\eta'(4\,^1S_0)$ are KK^*, $KK_1(1352)$, $KK_0^*(1430)$, $KK_0^*(1950)$ and the decay widths are much higher than the experimental data of BESIII. If we describe X(2370) as $\eta'(4\,^1S_0)$ with parameters in this work , it is obviously not appropriate.

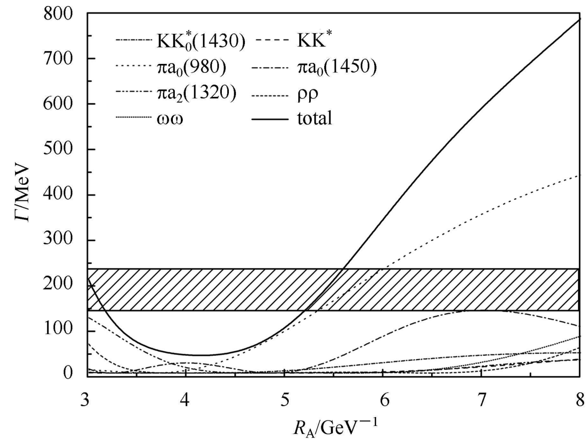

Fig. 6. The strong decay widths of the $\eta(4\,^1S_0)$.

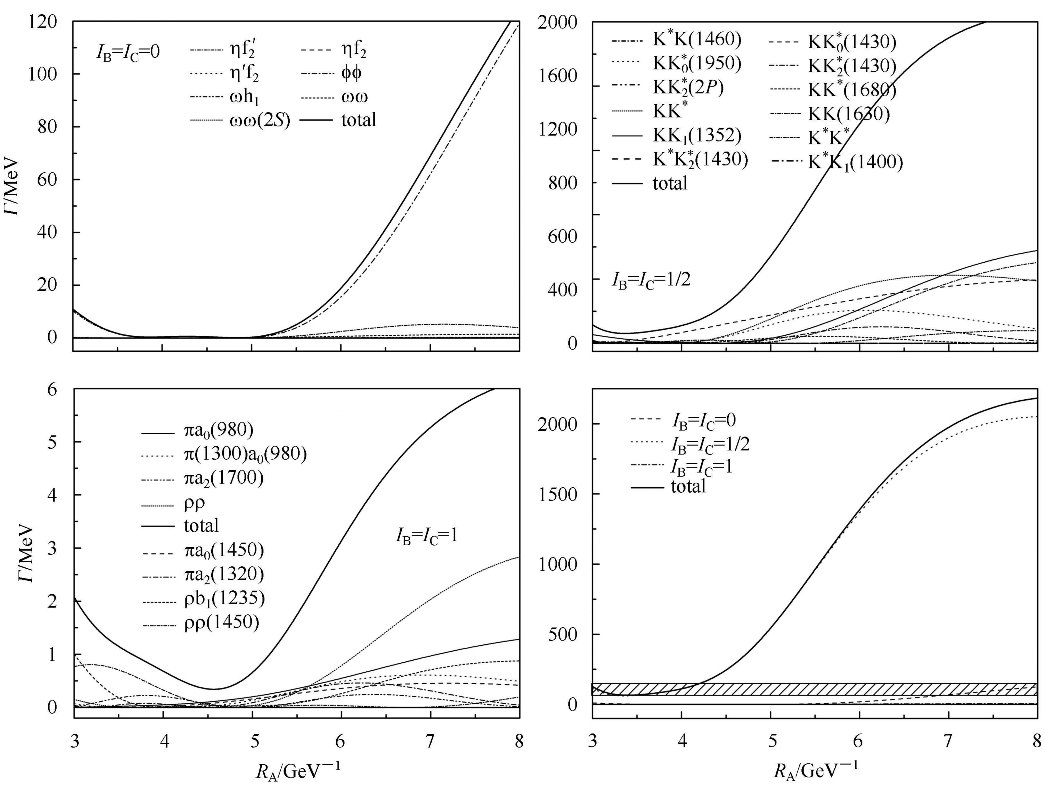

Fig. 7. The strong decay widths of the $\eta'(4\,^1S_0)$.

5 Summary and discussions

By using chiral quark model, the mass spectra of η and η′ families are calculated, where the mixing between $(u\bar{u}+d\bar{d})/\sqrt{2}$ and $s\bar{s}$ is determined by system dynamics, K-meson exchange. Based on the mass spectra, the possible candidates of four $J^{PC}I^{G}=0^{-+}0^{+}$ mesons, η(1760), X(1835), X(2120) and X(2370) are assigned to $\eta'(2^1S_0)$, $\eta(4^1S_0)$, $\eta'(3^1S_0)$, $\eta'(4^1S_0)$. Then all of their kinematically allowed two-body strong decays can be calculated within the framework of the $^3P_0$ model. The wavefunctions needed in the calculation are obtained from the mass calculation. To simplify the calculation, SHO wavefunctions are used to mimic real radial wavefunctions.

The decay widths turn out to be strongly dependent on the SHO wave function scale parameter β. For η(1760), the width is larger than the result of [6] but is compatible with the BES observation results [1] in the R_A range. However, the partial width to ωω is too small, which is incompatible with the experimental data [1, 3, 6]. So the assignment of η(1760) to $\eta(2^1S_0)$ is disfavored in the present calculation. For the state X(1835), the calculated decay width is consistent with the experimental data, and $\pi a_0(980)$ and $\pi a_0(1450)$ are the main decay modes. To justify the assignment, experimental investigation of the $\pi a_0(980)$ and $\pi a_0(1450)$ decay modes of X(1835) is needed. Sine X(1835) is around the threshold of $p\bar{p}$; it may be a mixture of $q\bar{q}$ and baryonium. Further study of state X(1835) by taking into account the mixture is essential to understand the nature of the state.

X(2120) and X(2370) are assigned to $\eta'(3^1S_0)$ and $\eta'(4^1S_0)$, respectively. Since they have larger masses, many strong decay modes are allowed and generally the phase space is large. The calculated total decay widths are much higher than the experimental values. The large decay width may be due to the overestimated value of γ. To exclude the impact of parameters, the branching ratio is better for justifying the assignment. More experimental data are needed. Since the lattice QCD predicts that the 0^{-+} glueball is about 2.3–2.6 GeV, which is around the masses of X(2120) and X(2370), the study with the mixture of $q\bar{q}$, glueball and other configurations are necessary to understand the nature of X(2120) and X(2370) states.

References

1 Ablikim M et al. (BES collaboration). Phys. Rev. Lett., 2005, **95**: 262001
2 Ablikim M et al. (BES collaboration). Phys. Rev. Lett., 2011, **106**: 072002
3 Baltrusaitis R M et al. (MARKIII collaboration). Phys. Rev. Lett., 1985, **55**: 1723–1726
4 Baltrusaitis R M et al. (MARKIII collaboration). Phys. Rev. D, 1986, **33**: 1222–1232
5 Bisello D et al. (DM2 collaboration). Phys. Lett. B, 1987, **192**: 239–244
6 Bisello D et al. (DM2 collaboration). Phys. Rev. D, 1989, **39**: 701–712
7 Ablikim M et al. (BES collaboration). Phys. Rev. D, 2006, **73**: 112007
8 Klempt E, Zaitsev A. Phys. Rep., 2007, **454**: 1–202
9 DING G J, YAN M L. Phy Rev. C, 2005, **72**: 015208; DING G J, YAN M L. Eur. Phys. J. A, 2006, **28**: 351–360
10 Dedonder J P, Loiseau B, El-Bennich B, Wycech S. Phys. Rev. C, 2009, **80**: 045207
11 WANG Z G, WAN S L. J. Phys. G, 2007, **34**: 505–512; WANG Z G. Eur. Phys. J. A, 2011, **47**: 71
12 LIU C. Eur. Phys. J. C, 2008, **53**: 413–419
13 Kochelev N, Min D P. Phys. Lett. B, 2006, **633**: 283–288; Phys. Rev. D, 2005, **72**: 097502
14 HE X G, LI X Q, LIU X, MA J P. Eur. Phys. J. C, 2006, **49**: 731–736
15 LI B A. Phys. Rev. D, 2006, **74**: 034019
16 HAO G, QIAO C F, ZHANG A L. Phys. Lett. B, 2006, **642**: 53–61
17 HUANG T, ZHU S L. Phys. Rev. D, 2006, **73**: 014023
18 LI D M, MA B. Phys. Rev. D, 2008, **77**: 074004
19 YU J S, SUN Z F, LIU X, ZHAO Q. Phys. Rev. D, 2011, **83**: 114007
20 Vijande J, Fernández F, Valcarce A. J. Phys. G, 2005, **31**: 481–506
21 LI X Q, Page P R. Eur. Phys. J. C, 1998, **1**: 579–583
22 WU N, YUAN T N, ZHENG Z P. HEP & NP, 2001, **10**: 611–612 (in Chinese)
23 Micu L. Nucl. Phys. B, 1969, **10**: 521–526
24 Yaouanc A Le, Oliver L, Pene O, Raynal J C. Phys. Rev. D, 1973, **8**: 2223–2234; 1974, **9**: 1415–1419; 1975, **11**: 1272–1286
25 Roberts W, Silvestr-Brac B. Few-Body Syst., 1992, **11**: 171–193
26 Ackleh E S, Barnes T, Swanson E S. Phys. Rev. D, 1996, **54**: 6811–6829
27 Jacob M, Wick G C. Ann. Phys. (N.Y.), 1959, **7**: 404–428
28 Manohar A, Georgi H. Nucl. Phys. B, 1984, **234**: 189–212
29 Koonin S E, Meredith D C. Computational Physics. New York: Addison-Wesley, 1990. 56–57
30 LU J, DENG W Z, CHEN X L, ZHU S L. Phys. Rev. D, 2006, **73**: 054012; ZHANG B, LIU X, DENG W Z, ZHU S L. Eur. Phys. J. C, 2007, **50**: 617–628; CHEN C, CHEN X L, LIU X, DENG W Z, ZHU S L. Phys. Rev. D, 2007, **75**: 094017
31 Blundell H G, Godfrey S. Phys. Rev. D, 1996, **53**: 3700–3711; Phys. Rev. D, 1996, **53**: 3712–3722
32 YANG Y C, XIA Z R, PING J L. Phys. Rev. D, 2010, **81**: 094003
33 Yaouanc A Le, Oliver L, Pene O, Raynal J C. Phys. Lett. B, 1977, **72**: 57–61
34 Nakamura K et al. J. Phys. G, 2010, **37**: 075021